Multistep magnetic switching in single-crystal (001)Co_2MnGe films

F. Y. Yang,[1] C. H. Shang,[1] C. L. Chien,[1] T. Ambrose,[2] J. J. Krebs,[2] G. A. Prinz,[2] V. I. Nikitenko,[1,3,4] V. S. Gornakov,[3,4] A. J. Shapiro,[3] and R. D. Shull[3]

[1]*Department of Physics and Astronomy, The Johns Hopkins University, Baltimore, Maryland 21218*

[2]*Code 6340, Naval Research Lab, 4555 Overlook Avenue, SW, Washington, D.C. 20375*

[3]*National Institute of Standards and Technology, Gaithersburg, Maryland 20899*

[4]*Institute of Solid State Physics, Russian Academy of Sciences, Chernogolovka, Russia 142432*

(Received 15 January 2002; revised manuscript received 21 February 2002; published 23 April 2002)

Multistep magnetic switching with single, double, and triple loops has been observed in single-crystal (001) Co_2MnGe Heusler alloy films epitaxially grown on GaAs (001) substrates due to a combined magnetic anisotropy consisting of cubic magnetocrystalline anisotropy and uniaxial anisotropy. Theoretical calculations of the hysteresis loops using coherent rotation show excellent agreement with the experimental results. Domain patterns and magnetization rotation in the Co_2MnGe films have been studied using the magneto-optical indicator film (MOIF) imaging technique. Magnetic domains and domain walls, as well as the coherent rotation of magnetization in single-step, double-step, and triple-step switching have been clearly observed. The magnetic switching field and domain wall pattern (90° and 180° domain walls) observed from the MOIF images are in excellent agreement with the results of the hysteresis measurements and the theoretical model.

DOI: 10.1103/PhysRevB.65.174410 PACS number(s): 75.60.−d, 75.70.−i, 68.55.−a, 75.50.−y

The availability of high-quality single-crystal thin films provides unique opportunities for the studies of the intrinsic magnetic anisotropy of ferromagnetic materials. Of particular interest is the interplay of uniaxial and cubic magnetocrystalline anisotropy in single-crystal thin films, in which one may observe a variety of switching characteristics with single, double, or even triple jumps. Of these, the magnetic switching behavior of single-crystal Fe and Fe alloy thin films has been most extensively studied.[1–13] Unfortunately, in most of the (100) oriented Fe films, the magnetic anisotropy is dominated by the cubic anisotropy with a miniscule uniaxial component, thus depriving the opportunity to observe the key features of combined magnetocrystalline and uniaxial anisotropy.

Heusler alloys are a group of ternary compounds consisting of full Heuslers (e.g., Co_2MnSi, Cu_2MnAl) and half-Heuslers (e.g., NiMnSn) first discovered a century ago.[14] Yet, there have been renewed interests in these materials because of their newly discovered properties. For example, some of the Heusler alloys have been predicted to be half-metallic ferromagnets (HMF),[15] in which there is only one spin band at Fermi energy and the other spin band is at a gap below the Fermi energy. The HMF's are therefore 100% spin polarized, with important technological implications in spin polarized transport.[16] Some Heusler alloys (e.g., Ni_2MnGa) also exhibit giant magnetostriction and shape memory effects.[17]

Co_2MnGe is one of the full-Heusler alloy with the potential of being highly spin polarized. In this paper, we report the unusual magnetic switching behavior of single-crystal Co_2MnGe (001) thin films which show single, double, and triple hysteresis loops. This behavior can be understood from a unique magnetic anisotropy, consisting of the cubic magnetocrystalline anisotropy of single-crystal Co_2MnGe(001) films and the (surface) uniaxial anisotropy of comparable magnitude due to the epitaxy with the underlying GaAs substrate.[2] We have developed a simple model that can quantitatively account for the unusual switching behavior. The magneto-optical indicator film (MOIF) imaging technique has been used to study the magnetic domains in single-crystal Co_2MnGe films. The MOIF images clearly show the proposed coherent rotation of magnetization. Furthermore, the MOIF images reveal domain wall propagation in such a system with unusual magnetic anisotropy. The MOIF results strongly support our explanation of the hysteresis process.

The (001)Co_2MnGe film, 250 Å in thickness, has been epitaxially grown on GaAs (001) substrates by molecular beam epitaxy (MBE).[18] Among other attributes, Co_2MnGe is one member of the Heusler alloys predicted to be a material with high spin polarization.[19] The structural properties of (001)Co_2MnGe films of cubic structure have been investigated using a four-circle x-ray diffraction system. The $\theta/2\theta$ scan of the film shows only the (00n) peaks with a lattice constant of $a=5.743$ Å. The rocking curve of the (004) peak of the Co_2MnGe film gives a full width at half maxima (FWHM) of 0.24°, which is essentially limited by the film thickness. The pole figure of Co_2MnGe (440) peak shows the fourfold symmetry at a tilt angle of 45°. The x-ray diffraction results demonstrate the high quality of the (001) Co_2MnGe film and its epitaxial relationship with the GaAs substrates, both are essential for the observation of the unusual switching behavior and the development of the theoretical model.

We have used vibrating sample magnetometry (VSM) to measure the hysteresis loops at room temperature with the magnetic field applied in the sample plane and at an angle β in 5° steps with respect to the [110] direction of Co_2MnGe, which is the easy axis of the film. Figures 1(a) and 2(a) show two representative hysteresis loops at $\beta=50°$ and 75°, respectively, displaying completely different switching behaviors. While a single hysteresis loop is observed at $\beta=50°$, as it is common for most ferromagnetic materials, the hysteresis loop at $\beta=75°$ consists of three separate loops. In addition to the main loop at the origin, there are two satellite loops

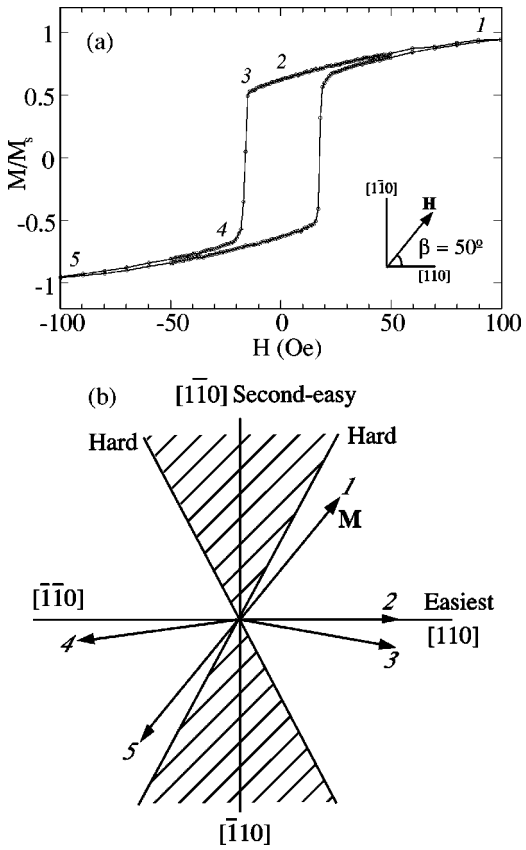

FIG. 1. (a) The hysteresis loop of a $(001)Co_2MnGe$ film with magnetic field **H** applied in the sample plane at $\beta=50°$ from the [110] axis, (b) the diagram illustrating the direction of **M** at five points on the hysteresis loop labeled in (a).

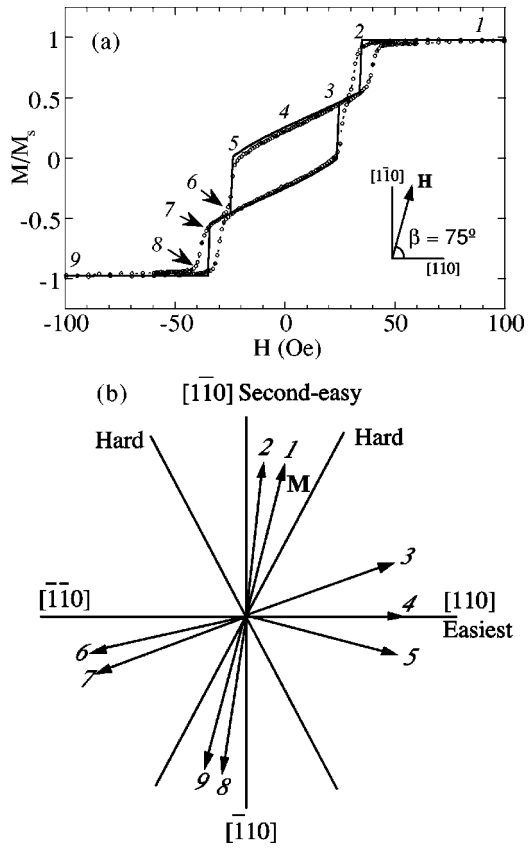

FIG. 2. (a) The hysteresis loop of a $(001)Co_2MnGe$ film with **H** applied in the sample plane at $\beta=75°$ and (b) the diagram illustrating the direction of **M** at nine points on the hysteresis loop labeled in (a). The open circles in (a) are the experimental data and the solid line in (a) is the calculated curve.

centered at $H=\pm 35$ Oe. For all angles, a single loop similar to Fig. 1(a) has been observed for $\beta\leqslant 60°$, whereas triple loops, such as that in Fig. 2(a), for $65°\leqslant\beta\leqslant 85°$. At $\beta=90°$, the center loop collapses with only two satellite loops remaining.

For the $(001)Co_2MnGe$ films, the groups of $\langle 110\rangle$ and $\langle 100\rangle$ axes are in the film plane. To understand the unusual switching behavior, it is essential to examine the consequence of two sources of magnetic anisotropy. The in-plane free energy density with combined cubic anisotropy and uniaxial anisotropy can be modeled as

$$E=K_1\alpha_1^2\alpha_2^2+K_u\sin^2\theta-\mathbf{H}\cdot\mathbf{M}, \tag{1}$$

where K_1 is the cubic anisotropy constant, α_1 and α_2 are the direction cosines with respect to the in-plane cubic [100] and [010] axes at $\alpha_1=\theta+45°$ and $\alpha_2=\theta-45°$. The factor K_u is the uniaxial anisotropy constant, θ the angle between magnetization **M** and the [110] axis, and last term is the Zeeman energy. One can calculate $E_{\rm an}/M_s$ as a function of θ, where $E_{\rm an}$ is the anisotropy energy and M_s the saturation magnetization, for cubic magnetocrystalline anisotropy [Fig. 3(b)], uniaxial anisotropy [Fig. 3(d)], and the combined anisotropy [Fig. 3(f)], by including the first, the second, and both terms, respectively, in Eq. (1). In Fig. 3(b), 3(d), and 3(f) and throughout this work, we have used $K_1/M_s=-33$ Oe and $K_u/M_s=20$ Oe, which provide quantitative agreement with the experimental results.

Including only the cubic magnetocrystalline anisotropy, $\langle 110\rangle$ are the easy axes, and $\langle 100\rangle$ the hard axes 45° away, as shown in Fig. 3(a). For uniaxial anisotropy alone, [110] is the easy axis, the hard $[1\bar{1}0]$ axis is 90° away, as shown in Fig. 3(c). However, in the $(001)Co_2MnGe$ films, while [110] is the easy axis, neither the [010] axis (45° away) nor the $[\bar{1}10]$ axis (90° away) is the hard axis. Furthermore, hysteresis loops of single, double, and triple loops have been observed.

Instead, in $(001)Co_2MnGe$, one has the rare occurrence of *combined* cubic magnetocrystalline anisotropy and uniaxial anisotropy with comparable magnitude sharing the *same* easy axis, where the latter is a (surface) uniaxial anisotropy due to epitaxy on the (001) zinc blende GaAs substrate.[2] As shown in Fig. 3(f), calculations including both types of anisotropy show that the [110] axis ($\theta=0°$) is the easiest axis with an energy minimum. The hard axis (marked by the vertical dashed line), with an energy maximum, is at $\theta=\frac{1}{2}\sin^{-1}(K_u/K_1)-45°=63°$, which comes about only when the uniaxial anisotropy is comparable with the cubic anisotropy. More interestingly, there is still *another* energy minimum at the $[1\bar{1}0]$ axis ($\theta=90°$), which is the second-

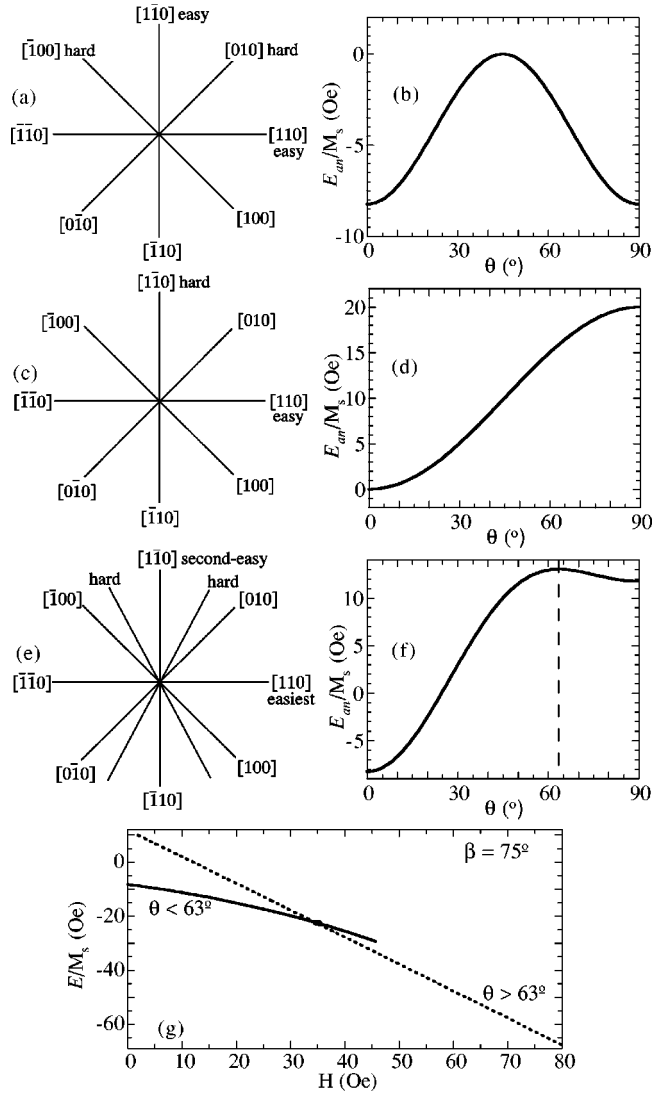

FIG. 3. Crystallographic directions of $(001)Co_2MnGe$ film, easy and hard axes for (a) cubic magnetocrystalline anisotropy, (c) uniaxial anisotropy, (e) combined anisotropy, and anisotropy energy as a function of θ, the angle between **M** and [110] axis, for (b) cubic magnetocrystalline anisotropy, (d) uniaxial anisotropy, (f) combined anisotropy. In (f), the dashed line marks the hard axis at $\theta=63°$. (g) The dependence of energy on magnetic field for $\beta=75°$. The dotted curve is for **M** at $\theta>63°$ and the solid curve is for **M** at $\theta<63°$.

easy axis. As indicated in Fig. 3(e), there are now one easiest axis ($\theta=0°$), one second-easy axis ($\theta=90°$), and two hard axes ($\theta=63°$ and 117°), a combination that gives rise to the unusual hysteresis loops.

For hysteresis loops at $0°\leqslant\beta<63°$, **M** always lies between the easiest axis and the hard axis, and the hysteresis loops are single loops. For the example in Fig. 1(a) with $\beta=50°$, the directions of magnetization at five representative points [1 through 5 in Fig. 1(a)] are shown in Fig. 1(b). At point 1, **M** is approximately parallel to **H**, i.e., $\theta\approx\beta=50°$. As H decreases, **M** rotates towards and passes the [110] easiest axis. At -16 Oe, **M** reverses abruptly to be near the $[\bar{1}\bar{1}0]$ axis at point 4, before being nearly parallel to **H** again at point 5. The entire process involves coherent rotation of magnetization and one nearly 180° switching. It should be noted that energetically there is no possibility for **M** to be oriented between the hard axis and the second-easy axis $[1\bar{1}0]$, indicated by the shaded sectors in Fig. 1(b).

For $63°<\beta\leqslant90°$, **M** could lie either between the hard axis and the second-easy axis or between the easiest axis and the hard axis depending on the magnitude of the magnetic field, resulting in the unusual multistep switching. Consider the example of $\beta=75°$ shown in Fig. 2(a). At point 1, **M** is approximately parallel to **H**, i.e., $\theta\approx\beta=75°$, as shown in Fig. 2(b). At point 2, just before the first jump, **M** coherently rotates towards $[1\bar{1}0]$, the second easy axis. From point 2 to point 3, **M** abruptly makes the first highly unusual nearly 90° switching to be near the [110] axis. As H decreases from point 3 to point 5, **M** coherently rotates towards, and passes the [110] axis until point 5. From point 5 to point 6, **M** switches to near $[\bar{1}\bar{1}0]$ via a nearly 180° switching. Between points 7 and 8, the third switching occurs with another nearly 90° switching as **M** switches to be near the $[\bar{1}10]$ axis. This switching and the first switching are symmetrical about the origin. At point 9, **M** is nearly aligned with **H** at $\theta\approx255°$. The whole process consists of coherent rotation of magnetization as a single domain, two nearly 90° switching and one nearly 180° switching events.

The highly unusual nearly 90° switching is due to a second-easy $[1\bar{1}0]$ axis, in addition to the easiest [110] axis. As H decreases to about 35 Oe near point 2 in Fig. 2(a), it is energetically more favorable for **M** to switch suddenly to be near the [110] axis than to continue rotating towards the $[1\bar{1}0]$ axis. This switching causes **M** to overcome the energy barrier of the hard axis and makes the nearly 90° switching. This is illustrated in Fig. 3(g) for $\beta=75°$, where the dotted and solid curves are for **M** to remain near the second-easy $[1\bar{1}0]$ axis and the easiest [110] axis, respectively. For $H>35$ Oe the dotted curve has the lower energy whereas at 35 Oe and below, the solid curve has the lower energy, thus **M** abruptly makes a near 90° switching to be close to the easiest [110] axis. One notes that the value of 35 Oe obtained in Fig. 3(g) is in good agreement with experimental results shown in Fig. 2(a).

Not only the rotation and switching of **M** can be described by Eq. (1), one can also quantitatively account for the measured hysteresis loops at all angles. The coherent rotation part of the hysteresis loops can be calculated from the free energy in Eq. (1). By minimizing E, $\partial E/\partial\theta=0$, we obtain

$$H=\frac{\sin(2\theta)}{\sin(\beta-\theta)}[K_u-2K_1\cos(\theta+45°)\cos(\theta-45°)]. \tag{2}$$

Since the measured value of magnetization is $M/M_s=\cos(\beta-\theta)$, one can obtain M vs H by eliminating θ. As an example, the solid curve in Fig. 2(a), which agrees well with experiment, is the calculated hysteresis loop using this method with $K_1/M_s=-33$ Oe and $K_u/M_s=20$ Oe for $\beta=75°$. A Stoner-Wohlfarth model, which does not constraint magentization to be in the thin film plane, could also produce

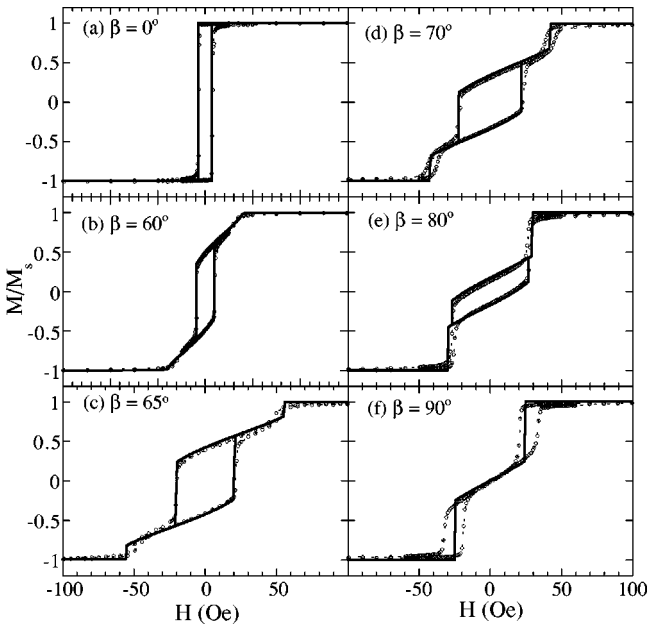

FIG. 4. The experimental (open circles) and calculated (solid lines) hysteresis loops of the Co_2MnGe film at $\beta=$(a) 0°, (b) 60°, (c) 65°, (d) 70°, (e) 80°, and (f) 90°.

the observed hysteresis but with a different set of anisotropy parameters. Since Eq. (2) does not accommodate irreversible hysteresis including coercivity, the switching fields of ± 25 Oe have been drawn in. The two satellite loops have been specified by two lines at ± 35 Oe, which have been calculated by minimizing the energy as mentioned above and shown in Fig. 3(g). The widths of the satellite loops and the hysteric nature of the two loops are due to the fact that **M** needs to overcome the energy barrier of the hard axis and the formation of domains and the propagation of domain wall during switching. These aspects can not be reproduced by Eq. (2).

Using the same values of $K_1/M_s=-33$ Oe and $K_u/M_s=20$ Oe and the method described above, we have calculated the hysteresis loops of $(001)Co_2MnGe$ at all angles (β) with only coherent rotation. As shown in Fig. 4, the experimental results are shown as open circles and the calculated curves are shown as solid curves. For the hysteresis loops at $\beta<63°$, as concluded earlier, there is only one loop due to coherent rotation and one near 180° switching. As β increases from 0° to 60°, the hysteresis loops become more slanted, which is typical for ferromagnets with uniaxial anisotropy. At $\beta>63°$, triple loops are observed. The two satellite loops becomes more prominent as β approaches 90° because the switching angle of **M** increases with β. At $\beta=90°$, the switching angle is close to 90°, and the central loop collapses, similar to the hysteresis loop measured with **H** perpendicular to the easy axis in magnetic films with uniaxial anisotropy.[18] The excellent agreement between the experimental data and calculated hysteresis loops in Fig. 4 for all values of β attests to the fact that the simple model is suitable for the understanding of the hysteresis process of the Co_2MnGe films.

It is important to stress that combined cubic magnetocrystalline anisotropy and uniaxial anisotropy with comparable strength and sharing the same easy axis is rarely realized experimentally. It requires a single-crystal ferromagnetic film with cubic anisotropy epitaxially grown on a single-crystal substrate, which incorporates a uniaxial anisotropy in the ferromagnetic film with the same easy axis. These stringent conditions have been realized in the $(001)Co_2MnGe$ film, epitaxially grown on (001)GaAs. Previously, two-jump switching has been reported in epitaxial Fe thin films due to the cubic anisotropy.[3–6] Hathaway *et al.* observed a three-step switching in Fe films at 7° and 12° from the hard axis [110] and attributed it to the demagnetizing effect.[1] Cowburn *et al.* reported a hysteresis loop with three jumps in ultrathin Fe film with cubic anisotropy and a weak uniaxial anisotropy.[7] They attributed the multijump switching to domain wall pinning and the weak uniaxial anisotropy. Coherent rotation was not taken into account and **M** was assumed to lie on the four easy directions of the cubic axes. Based on their calculation, three-jump switching can only be observed in a narrow range of angle when K_u is greater than the domain wall pinning energy.[7] For the Co_2MnGe films we studied, the uniaxial anisotropy energy is much larger than that in epitaxial Fe films reported previously. In this work, we have the opportunity to clearly observe the three-step switching from 63° up to nearly 90° in these films. We have quantitatively shown coherent rotation of magnetization rather than along the four easy axes as previously assumed.[7] In addition, two nearly 90° switchings at $\beta>63°$ have been observed and theoretically accounted for.

The MOIF imaging technique provides a powerful tool to investigate the domain wall pattern as well as the magnetization rotation.[20] In the MOIF technique, a Bi-substituted iron garnet film (indicator) with an Al underlayer was placed on top of the sample. A polarized light is focused by a microscope on the Al underlayer through the indicator film and reflected back. The polarization of the light experiences a Faraday rotation in the indicator film. When the microscope polarizers are slightly uncrossed, the variations of the brightness of the image represent the variations of the stray field component perpendicular to the indicator film. Thus, any magnetization discontinuities in the sample, such as the edges, ferromagnetic (FM) domain walls, and defects, can be observed in the indicator film. The magnetization **M** of a ferromagnetic domain points from the ''black'' edge towards the ''white'' edge shown in the MOIF images. MOIF imaging is very suitable for the study of domain pattern and the rotation of magnetization.

We have used the MOIF technique to observe the domain pattern of the $(001)Co_2MnGe$ film at different field angles of β. We focused the microscope on an area of 1 mm $\times 1.3$ mm near the upper right corner of the sample. We will discuss the MOIF results at four representative field angles $\beta=0°, 90°, 55°$, and $-75°$ below.

The hysteresis loop in Fig. 5 is for the magnetic field parallel to the easiest axis ($\beta=0°$). Six MOIF images [Figs. 5(a) to 5(f)], taken at six points (a,b,c,d,e,f) in the hysteresis loop, are shown above the hysteresis loop. The easiest axis [110] is along the horizontal direction in the MOIF images. The applied magnetic field is parallel to the easiest axis

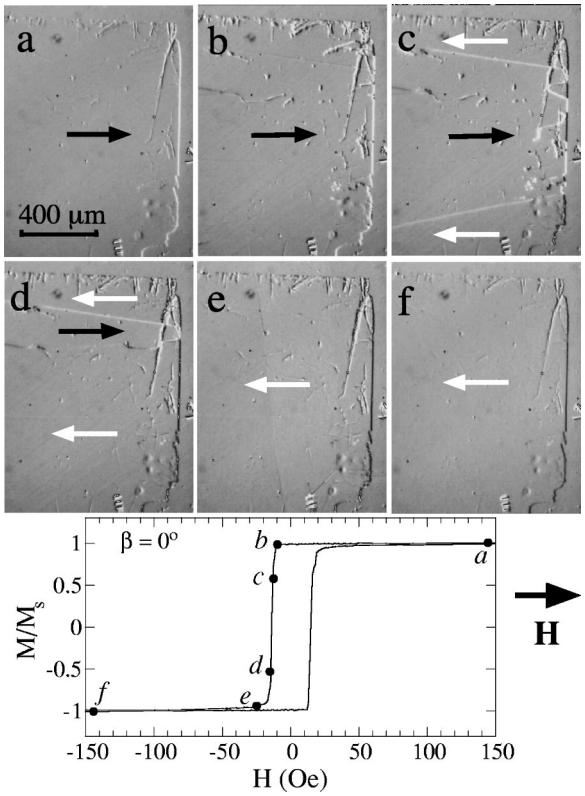

FIG. 5. The MOIF images of the (001)Co_2MnGe film with **H** parallel to the easiest axis ($\beta=0°$). The hysteresis loop is shown below. The easiest axis is horizontal and direction of the magnetic field is illustrated on the right of the hysteresis loop. The six points marked in the hysteresis loop indicate where the images were taken: (a) $H=150$ Oe, (b) $H=-10$ Oe, (c) $H=-12$ Oe, (d) $H=-15.6$ Oe, (e) $H=-24$ Oe, (f) $H=-150$ Oe.

with the positive direction pointing to the right. The arrows in the MOIF images indicate the magnetization directions.

Corresponding to point *a* in the loop, where **M** is aligned with **H**, the black arrow in Fig. 5(a) also shows that **M** is parallel to **H**. That **M** points from left to right is indicated by the white contrast at the right edge of the sample. At point *b*, with $H=-10$ Oe just before the jump, the film is still a single domain with **M** pointing to the right. At point *c* with $H=-12$ Oe, where **M** began to reverse, stripe domains with domain walls nearly parallel to the easiest axis in Fig. 5(c). The white arrows in the stripe domains indicate that they are the intruding domains, whose magnetizations point to the left. As $H=-15.6$ Oe at point *d*, the domains with **M** pointing to the left (white arrows) become larger at the expense of domains with **M** pointing to the right (black arrows), accommodated by domain walls propagating perpendicular to the easiest axis. At $H=-24$ Oe (point *e*) and at even more negative *H* (point *f*), the whole film becomes a single domain with **M** pointing to the left. The right edge in Figs. 5(e) and 5(f) becomes black, indicating **M** is pointing towards the left edge. Figure 5(f) appears ''smoother'' than Fig. 5(e) because of fewer defects that require higher fields to switch. It is clear that in the whole hysteresis process **M** completes a 180° switching, similar to that in ferromagnetic films with just uniaxial anisotropy.

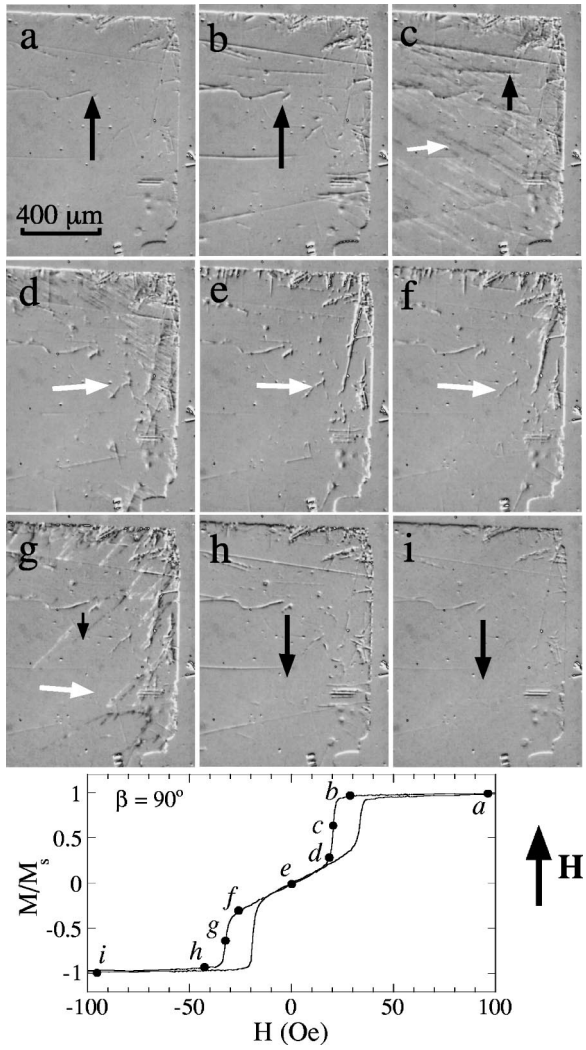

FIG. 6. The MOIF images of the (001)Co_2MnGe film with **H** parallel to the second-easy axis ($\beta=90°$). The easiest axis is horizontal. The nine points marked in the hysteresis loop in the lower part indicate where image (a) to (i) were taken: (a) $H=100$ Oe, (b) $H=29$ Oe, (c) $H=20$ Oe, (d) $H=18$ Oe, (e) $H=0$ Oe, (f) $H=-27$ Oe, (g) $H=-31$ Oe, (h) $H=-42$ Oe, (i) $H=-100$ Oe. The direction of the magnetic field is illustrated on the right of the hysteresis loop.

When **H** is applied parallel to the second easy axis at $\beta=90°$, there are two loops in the hysteresis loop [Fig. 4(f)]. Figure 6 shows nine MOIF images taken at $\beta=90°$, as *H* is swept from positive to negative. In the MOIF images in Fig. 6, the second easiest axis is vertical and the positive direction of the magnetic field is up, as indicated by the single-domain image shown in Fig. 6(a), and the white contrast at the top edge. As *H* decreases to about 29 Oe at point *b*, just before the first jump, **M** still points to the top edge as shown in Fig. 6(b). The right edge of the sample in Fig. 6(b) becomes whiter because the magnetization near the edge tends to switch first before the entire film. As *H* further decreases to 20 Oe at point *c* in the middle of the first jump, stripe domain walls that have an angle about 30° with the easiest axis can be seen in Fig. 6(c). The intruding domains (marked by white arrow) have a magnetization approximately pointing to the

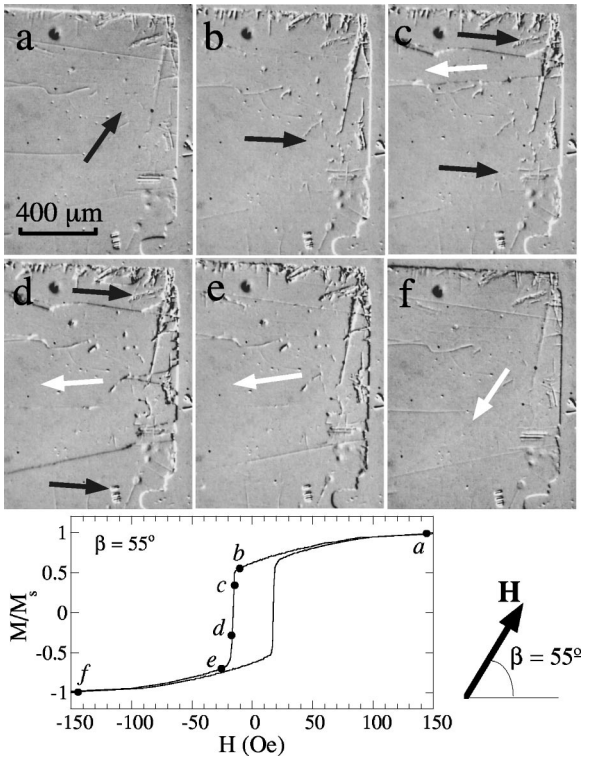

FIG. 7. The MOIF images of the (001)Co_2MnGe film at $\beta = 55°$. The easiest axis is along the horizontal direction. The six points marked in the hysteresis loop in the lower part indicate where image (a) to (f) were taken: (a) $H = 150$ Oe, (b) $H = -12$ Oe, (c) $H = -17$ Oe, (d) $H = -18$ Oe, (e) $H = -25$ Oe, (f) $H = -150$ Oe. The direction of the magnetic field is illustrated on the right of the hysteresis loop.

right. The white arrow tilts a few degrees towards the top due to the applied magnetic field (20 Oe). At point *d* just after the first jump ($H = 18$ Oe), the whole film essentially becomes a single domain with **M** pointing to the right. Therefore, from *a* to *d*, **M** rotates about 90° during the switching.

At $H = 0$ Oe (point *e*), the whole film is a single domain with magnetization pointing right and parallel to the easiest axis [Fig. 6(d)]. Ideally, if **H** is exactly parallel to the second-easy axis, the film should break up into multiple domains at $H = 0$ Oe. But in reality, the applied magnetic field is off the second-easy axis one way or the other, resulting in a preferred orientation of magnetization at zero field (''right'' in this case). When *H* decreases to the negative side at point *f* just before the second jump ($H = -27$ Oe), the film is still a single domain. In Fig. 6(f), **M** approximately points right and bends downwards by a few degrees due to the magnetic field. At point *g* in the middle of the second jump ($H = -31$ Oe), intruding domains with domain walls at an angle about 45° with the easiest axis were observed in Fig. 6(g). The magnetization in these intruding domains follows the field direction and points down. The domain wall orientation of the intruding domains in Fig. 6(g) is approximately perpendicular to that in Fig. 6(c). This originates from the fact that **M** rotates from up to right during the first jump and from right to down during the second jump. At point *h* just after the second jump, the film forms a single domain with **M**

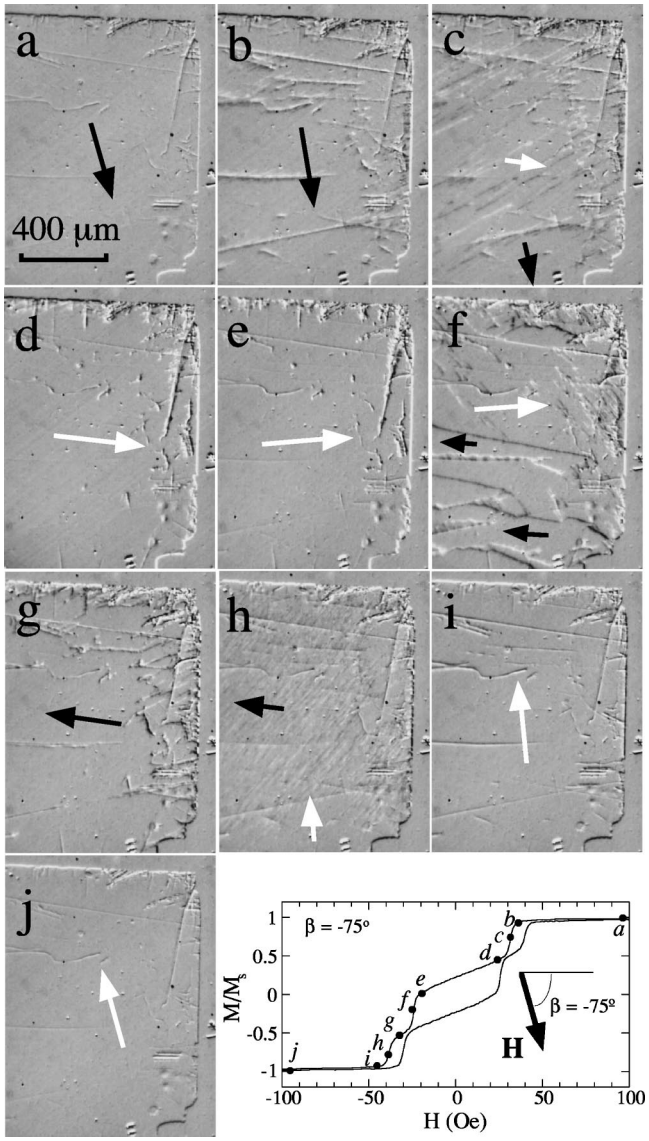

FIG. 8. The MOIF images of the Co_2MnGe film at $\beta = -75°$. The easiest axis is horizontal direction. The ten images were taken at (a) $H = 100$ Oe, (b) $H = 35$ Oe, (c) $H = 30$ Oe, (d) $H = 24$ Oe, (e) $H = -20$ Oe, (f) $H = -24$ Oe, (g) $H = -32$ Oe, (h) $H = -39$ Oe, (i) $H = -46$ Oe, (j) $H = -100$ Oe. The hysteresis loop in the lower part indicate the ten points where the images were taken. The direction of the magnetic field is illustrated on the right of the hysteresis loop.

pointing down. At point *i* when *H* was very large in the negative side, the domain pattern is the same as that in Fig. 6(h), except that Fig. 6(i) looks ''smoother.'' From point *a* to *i*, **M** reversed its orientation by two ~90° switching.

We next examine the MOIF images with **H** applied between the easiest and the hard axes at $\beta = 63°$. At $\beta = 55°$, just a few degrees before reaching the hard axis at $\beta = 63°$, there is only one jump in the hysteresis loop, as shown in Fig. 7. When *H* is vary large at point *a*, **M** is saturated along the field direction, as shown in Fig. 7(a). Both the top and the right edges are white, indicating **M** is at an angle with both edges and pointing towards them. As *H* decreases to −12 Oe at point *b*, **M** is essentially along the easiest axis (horizontal)

and points right (the right edge becomes whiter). From point *a* to *b*, **M** coherently rotates about 55° from being parallel to **H** to along the easiest axis. At point *c* ($H=-17$ Oe), **M** starts to reverse. An intruding domain marked with a white arrow near the top edge of the sample was observed in Fig. 7(c). The position and the shape of the intruding domain is very close to that in Fig. 5(d) because in both cases, **M** reverses essentially along the easiest axis. When *H* became smaller at point *d* ($H=-18$ Oe), the intruding domain grows larger, as shown in Fig. 7(d). At point *e* just after **M** finished reversal ($H=-25$ Oe), the film became a single domain (except the tiny area near the edges and defects). As *H* decreased further to nearly -150 Oe at point *f*, **M** coherently rotates towards the field direction and is parallel to **H** at point *f*. It is clearly seen that the top and right edges in Fig. 7(f) are black, opposite to those in Fig. 7(a), indicating that **M** has reversed its direction from point *a* to *f*. The entire hysteresis process includes one $\sim 180°$ switching and coherent rotation of **M**.

The most unusual switching behavior of this single-crystal Co_2MnGe film is that it displays a three-step switching at $63° < \beta < 90°$. Figure 8 shows ten MOIF images taken at positions marked in the hysteresis loop at $\beta=-75°$, which has the same characteristics as that at $\beta=75°$, due to symmetry. When *H* is large in the positive direction (point *a*), **M** is parallel to **H**, as shown in Fig. 8(a). At point *b* ($H=35$ Oe), just before the first switching, the whole film is still a single domain, except that, **M** rotates towards the second-easy axis (vertical) by a few degrees. This is because the Zeeman energy ($-\mathbf{H}\cdot\mathbf{M}$) increases as *H* decreases from 100 to 35 Oe. As a result, **M** rotates towards magnetically easier direction, the second-easy axis. The lines in Fig. 8(b) indicate the defects in the film, where **M** differs from the large area of the film. At point *c* in the middle of the first switching ($H=30$ Oe), stripe domains at an angle about 30° with the easiest axis are observed in Fig. 8(c). The magnetization in these intruding domains is approximately along the easiest axis and pointing to the right. At point *d* ($H=24$ Oe), just after the first jump, the whole film becomes a single domain with **M** pointing essentially to the right. The slight downward of **M** in Fig. 8(d) is due to the small field ($+24$ Oe) applied at $\beta=-75°$. Thus, during the first switching, **M** rotates nearly 90° from near the second-easy axis to near the easiest axis.

From point *d* to *e*, **M** coherently rotates in counterclockwise direction. And the rotation of **M** by a small angle can be clearly seen by comparing the top edge in Figs. 8(d) and 8(e). The top edge changes from somewhat black in Fig. 8(d) to somewhat white in Fig. 8(e), indicating that **M** rotates from downwards [Fig. 8(d)] to upwards [Fig. 8(e)]. As *H* decreases to -24 Oe at point *f*, intruding domains with **M** pointing to the left are observed in Fig. 8(f). Due to the moderate field strength, the magnetization in all domains is slightly off the easiest axis. At point *g* ($H=-32$ Oe) between the second and the third switching, most area of the film has already reversed. From point *e* to *g*, **M** switches by nearly 180°. At point *h* ($H=-39$ Oe), stripe domains at an angle about 45° with the easiest axis can be seen in Fig. 8(h). This is another 90° switching and **M** is pointing up in these stripe domains. At point *i*, just after the third jump, the film becomes a single domain with **M** close to the second-easy axis. As *H* becomes very large in the negative direction, **M** is aligned with the field at point *j*. Therefore, from point *a* to *h*, **M** has two near 90° switching and one near 180° switching in a half cycle of the hysteresis loop.

It is particularly useful to compare the magnetization directions deduced from the theoretical model as shown Fig. 2(b), and the actual directions as indicated by the MOIF images shown in Figs. 8(a)–8(j). The magnetization directions (1,2, . . . ,8,9) in Fig. 2(b) have been obtained from the theoretical model that can reproduce the hysteresis loop in Fig. 2(a). The actual domain observation as shown in Figs. 8(a)–8(j) confirms these magnetization directions during the entire hysteretic process.

In summary, a combined cubic anisotropy and uniaxial anisotropy has been realized in single-crystal (001)Co_2MnGe films epitaxially grown on (001)GaAs substrates. As a result, within the film plane, there are one easiest axis [110] ($\theta=0°$), one second-easy axis [$1\bar{1}0$] ($\theta=90°$), and two hard axes ($\theta=63°$ and 117°). We have observed single-loop, two-loop, and unusual three-loop switching behavior when the magnetic field has been applied at angle β with the [110] axis. A simple model can numerically account for the results at all angles. Domain patterns in the Co_2MnGe films have been clearly observed using the MOIF technique. The MOIF images reveal near 90° and near 180° switching, as well as the coherent rotation of magnetization at various directions of the magnetic field. The MOIF imaging results are in excellent agreement with the theoretical model.

This work was supported by NSF Grant No. DMR01-01814.

[1] K. B. Hathaway and G. A. Prinz, Phys. Rev. Lett. **47**, 1761 (1981).
[2] J. J. Krebs, B. T. Jonker, and G. A. Prinz, J. Appl. Phys. **61**, 2596 (1987).
[3] J. M. Florczac and E. Dan Dahlberg, Phys. Rev. B **44**, 9338 (1991).
[4] J. R. Childress, R. Kergoat, O. Durand, J.-M. George, P. Galtier, J. Miltat, and A. Schuhl, J. Magn. Magn. Mater. **130**, 13 (1994).
[5] C. Daboo, R. J. Hicken, D. E. P. Eley, M. Gester, S. J. Gray, A. J. R. Ives, and J. A. C. Bland, J. Appl. Phys. **75**, 5586 (1994).
[6] R. P. Cowburn, S. J. Gray, J. Ferr, J. A. C. Bland, and J. Miltat, J. Appl. Phys. **78**, 7210 (1995).
[7] R. P. Cowburn, S. J. Gray, and J. A. C. Bland, Phys. Rev. Lett. **79**, 4018 (1997).
[8] H. C. Mireles and J. L. Erskine, J. Appl. Phys. **89**, 6671 (2001).
[9] A. F. Isakovic, J. Berezovsky, P. A. Crowell, L. C. Chen, D. M. Carr, B. D. Schultz, and C. J. Palmstrøm, J. Appl. Phys. **89**, 6671 (2001).

[10] O. Hellwig, J. B. Kortright, K. Takano, and E. E. Fullerton, Phys. Rev. B **62**, 11 694 (2000).
[11] J. A. C. Bland, M. J. Baird, H. T. Leung, A. J. R. Ives, K. D. Mackay, and H. P. Hughes, J. Magn. Magn. Mater. **113**, 178 (1992).
[12] W. Weber, C. H. Back, A. Bischof, A. Pescia, and R. Allenspach, Nature (London) **374**, 788 (1995).
[13] F. Y. Yang, C. L. Chien, X. W. Li, A. Gupta, and Gang Xiao, Appl. Phys. Lett. **77**, 286 (2000).
[14] F. Heusler, Verh. Dtsch. Phys. Ges. **5**, 219 (1903).
[15] R. A. de Groot, F. M. Mueller, P. G. van Engen, and K. H. J. Buschow, Phys. Rev. Lett. **50**, 2024 (1983).
[16] G. A. Prinz, Science **282**, 1660 (1998).
[17] K. Ullakko, J. K. Huang, C. Kantner, V. V. Kokorin, and R. C. O'Handley, Appl. Phys. Lett. **69**, 1966 (1996).
[18] T. Ambrose, J. J. Krebs, and G. A. Prinz, Appl. Phys. Lett. **76**, 3280 (2000).
[19] S. Ishida, S. Fujii, S. Kashiwagi, and S. Asano, J. Phys. Soc. Jpn. **64**, 185 (1995).
[20] V. I. Nikitenko, V. S. Gornakov, L. M. Dedukh, Yu. P. Kabanov, A. F. Khapikov, A. J. Shapiro, R. D. Shull, A. Chaiken, and R. P. Michel, Phys. Rev. B **57**, R8111 (1998).